Ecological Informatics 5 (2010) 367–378

Contents lists available at ScienceDirect

Ecological Informatics

journal homepage: www.elsevier.com/locate/ecolinf

A study on the relationship between Atlantic sea surface temperature and Amazonian greenness

Jaeil Cho [a,*], Pat J.-F. Yeh [b], Yang-Won Lee [c], Hyungjun Kim [b], Taikan Oki [b], Shinjiro Kanae [d], Wonsik Kim [e], Kyoichi Otsuki [a]

[a] Kasuya Research Forest, Kyushu University, Sasaguri, Fukuoka 811-2415, Japan
[b] Institute of Industrial Science, The University of Tokyo, 4-6-1 Komaba, Meguro-ku, Tokyo 153-8505, Japan
[c] Department of Geoinformatic Engineering Sciences, Pukyong National University, Busan, 608-737, Republic of Korea
[d] Department of Mechanical and Environmental Informatics, Tokyo Institute of Technology, 2-12-1 O-okayama, Meguro-ku, Tokyo 152-8552, Japan
[e] National Institute for Agro-Environmental Sciences, 3-1-3 Kannondai, Tsukuba 305-8604, Japan

ARTICLE INFO

Keywords:
Amazonia NDVI
Atlantic SST
Climate change

ABSTRACT

The growth of tropical rainforest in Amazon is critically vulnerable to the change in rainfall and radiation than in temperature, and that amount of rainfall and cloudiness in the northeast region of South American is strongly affected by the Atlantic sea surface temperature (SST). Results from recent model experiments for future climate projection have indicated a reduction of Amazonian greenness by a weakening of tropical vapor circulation system related with the change in SST. Therefore, the observational investigation of the relations between the Amazon greenness and Atlantic SST is fundamental to understand the response of Amazonian tropical forest to climate change. In this study, the effect of Atlantic SST on the spatial and temporal change of the Normalized Difference Vegetation Index (NDVI) in the Amazonian region is examined by using satellite remote sensing data for the period of 1981–2001. A strong correlation between NDVI and SST is found for certain regions in Amazon during the periods of 1980s and 1990s, respectively. In addition, strong correlations with NDVI lagging behind SST for two months and one year, respectively, are also identified from the interannual December-to-February (rain season) variations during 1981–2001. Despite these findings, the mechanisms behind the identified correlation remain unclear. Further analyses using observed precipitation and radiation data are required to understand the potential changes of Amazonian rainforest in the context of global warming.

1. Introduction

Tropical Amazon region, containing 70–80 billion metric ton (10^{15} ton) of carbon in plant biomass, is one of the largest plant ecosystems on the Earth and its biomass richness plays a critical role on the global carbon and water cycles (Cox et al., 2000). However, plant ecosystem in the Amazonia is vulnerable to environmental changes. Regional climate variability in this area has thus a large impact on the global carbon and water budget through the physiological and phonological changes of vegetation (Bonan, 2002).

The rapid global warming in atmospheric circulation pattern may lead to unexpected climate changes (IPCC, 2007). However, the response of vegetation processes (e.g., sustainability, decline and resilience) under climate change in tropical forest has not yet been fully understood (Lovejoy and Hannah, 2004; Bonan, 2002). For example, several climate model simulations coupled with dynamic vegetation processes have consistently forecasted the transition from tropical forest to savanna in Amazon under higher temperature and more frequent drought occurrence under future climate change (Cox et al., 2004; Marengo et al., 2001).

Compared to vegetations in the northern Asia, America and Europe, tropical plant ecosystems are more sensitive to the fluctuations of available soil moisture and absorbed radiation energy than temperatures (Myneni et al., 1996; Nemani et al., 2003; Huete et al., 2006). Soil water and radiation are closely dependent on atmospheric conditions such as cloudiness. The cloud amount in the tropical areas located near the ocean are significantly affected by sea surface temperature (SST), which can modify the pattern and intensity of atmospheric moisture transport to the land regions (Knight et al., 2006; Good et al., 2008). Therefore, the spatio-temporal variability of SST is one of the potential main drivers to influence the variability of tropical vegetation (Cox et al., 2004; Li et al., 2007).

The influence of SST on vegetation greenness, as detected by remotely sensed Normalized Difference Vegetation Index (NDVI), has been reported previously. Myneni et al. (1996) showed that the NDVI in the northeastern Brazil, where savanna is the dominant vegetation

* Corresponding author. Tel.: +81 92 948 3104 (office); fax: +81 92 948 3119.
E-mail address: chojaeil@forest.kyushu-u.ac.jp (J. Cho).

1574-9541/$ – see front matter © 2010 Elsevier B.V. All rights reserved.
doi:10.1016/j.ecoinf.2010.05.005

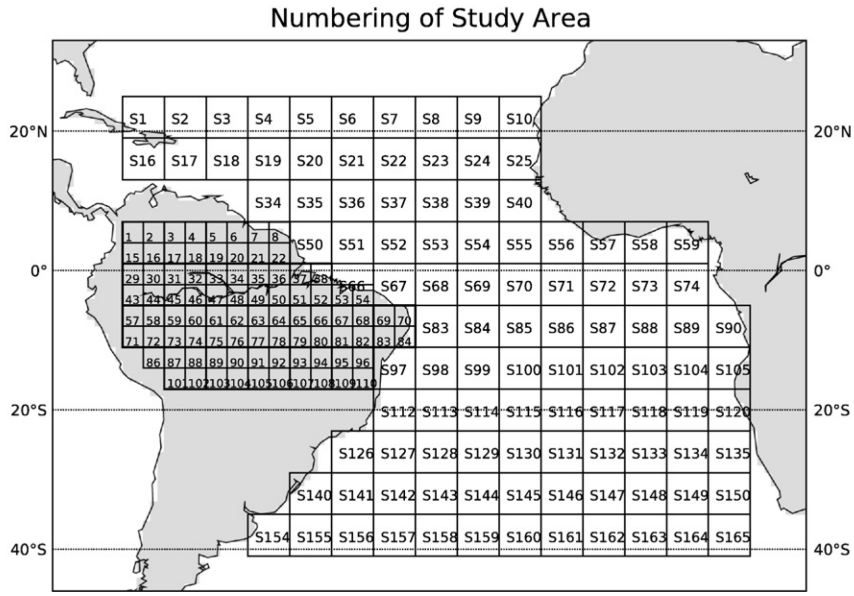

Fig. 1. Grid box numbering in the study area of Amazon and Atlantic Ocean. Land (L) has in total 87 grid boxes, while Sea (S) has in total 105 grid boxes.

type, has a negative correlation with the Eastern Tropical Pacific (Nino-3 region; 5°N-5°S by 90°W-150°W) SST anomalies during the warm and cool phases of ENSO (El Niño-Southern Oscillation) events. Los et al. (2001) studied the co-variability between NDVI, precipitation, temperature and SST during 1980s on the global scale. They found strong ENSO signals in the northeastern Brazil in terms of the anomalies of NDVI, precipitation and temperature.

However, the relations between the NDVI of Amazon rainforest and SST in the part of Atlantic Ocean adjacent to Amazon have rarely been investigated in previous studies, owing to the fact that the identification of their explicit relationships may require extensive investigations among most of influencing factors, such as rainfall and radiation. Firstly, Amazon rainforest, constructed by an enormous amount of biomass and biodiversity, has a complex response to environmental change. Indeed, a variety of major environmental factors have been recognized to influence the Amazon rainforest. During its rainy season, Amazon forest is not under soil moisture stress; rather the radiation is the limiting factor for plant growth. To the contrary, soil moisture decreases in dry season whereas radiation increases. Amazon rainforest thus experiences different environmental stress in different seasons. Flux measurement data reported by Saleska et al. (2003) indicated that more carbon uptake by the Amazon forest in dry season than rain season, and the satellite remote sensing data collected by Huete et al. (2006) reported a "greening up" during dry season, since about half of the trees in Amazon rainforest can rely on their deep root systems to overcome water stress in dry season (Nepstad et al., 1994). However, long-term monitoring data for the above-ground biomass reported by Phillips et al. (2009) revealed that extreme drought as happened in 2005 led to the decreased biomass in Amazonia.

Secondly, most of the previous investigations on linking Amazon rainfall to SST have focused on the influence of ENSO (Enfield, 1996; Knight et al., 2006; Harris et al., 2008). From the perspective of climate modelling, the control of ENSO on the Amazon rainfall is via the warming of Pacific Ocean SST driven by the change in wind and ocean–atmosphere heat exchange. However, the influence of Atlantic SST on Amazon rainfall has been found critical when ENSO is typically weak (Zeng et al., 2008), since the tropical Atlantic Ocean plays a critical role in determining the position of the intertropical convergence zone (ITCZ) which significantly affects the rainfall in equatorial regions (Enfield, 1996). Previous climate model studies (Knight et al., 2006; Harris et al., 2008) have also shown that the relative warming in the north tropical Atlantic Ocean can cause drying over the part of Amazon region south to the equator. Although the significance of Pacific Ocean (ENSO) on the Amazon rainfall has been well recognized (Ronchail et al., 2002), the Atlantic Ocean can also have an influence on Amazon rainfall. Enhanced rainfall conditions in Amazon are associated with an increase of water vapor transport from the Atlantic Ocean (Marengo, 1992; Rao et al., 1996), thus a close correspondence between the NDVI in Amazon and Atlantic SST can be reasonably expected (Zeng et al., 2008).

The heterogeneity of vegetation physiological characteristics and the complexity of ocean–atmosphere interactions may complicate the correlation between the Amazon NDVI and the Atlantic SST. For example, in addition to having a deep root system to overcome soil water stress, several field studies also reported that Amazonian forest canopies respond to seasonal droughts by an increase in litterfall by 10–35% (Smith et al., 1998). Moreover, the sources of moisture advection into the Amazon region, and hence the exact locations where SST influences Amazon rainfall, are not easy to be determined (Eagleson, 1986). It has been found (Zeng et al., 2008) that by

Table 1
The definition of 22 general land cover types from the GLC2000 project (IGBP, 1997).

Value	Class names
1	Tree Cover, broadleaved, evergreen
2	Tree Cover, broadleaved, deciduous, closed
3	Tree Cover, broadleaved, deciduous, open
4	Tree Cover, needle-leaved, evergreen
5	Tree Cover, needle-leaved, deciduous
6	Tree Cover, mixed leaf type
7	Tree Cover, regularly flooded, fresh water
8	Tree Cover, regularly flooded, saline water
9	Mosaic: Tree Cover/other natural vegetation
10	Tree Cover, burnt
11	Shrub Cover, closed–open, evergreen
12	Shrub Cover, closed–open, deciduous
13	Herbaceous Cover, closed–open
14	Sparse herbaceous or sparse shrub cover
15	Regularly flooded shrub and/or herbaceous cover
16	Cultivated and managed areas
17	Mosaic: Cropland/Tree Cover/other natural vegetation
18	Mosaic: Cropland/Shrub and/or grass cover
19	Bare areas
20	Water bodies
21	Snow and ice
22	Artificial surfaces and associated areas

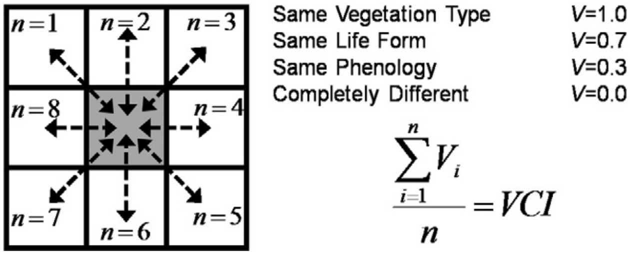

Fig. 2. VCI (Vegetation Complexity Index) computed from the average closeness value (V) of eight neighboring pixels of a certain pixel (in gray). The value of V is given in Table 2. ($n = 8$).

combining the influences of both tropical Pacific and Atlantic SST, 53% of rainfall variability in Amazon can be explained, which is higher than only one SST is considered. Despite substantial complexities involved, Atlantic SST exerts a distinct influence on the climate of Amazon that is comparable to its well-known Pacific SST linkage (Zeng et al., 2008). Thus, the investigation on the feasibility of using Atlantic SST to predict Amazonian greenness is important for the understanding of global carbon cycle under climate change.

In this study, we evaluate the feasibility of using Atlantic SST for understanding seasonal variability of Amazon vegetation by examining the temporal and spatial correlation between the NDVI in Amazon and Atlantic SST. To our knowledge, similar investigations on linking Atlantic SST to Amazonian greenness have not yet been reported in literature. Section 2 describes the satellite remote sensing imagery data and the methodology used in this study. Section 3 provides an overview on the characteristics and past variations of Amazonian NDVI and Atlantic SST before examining their relationships. The analyzed results based on remote sensing data are presented and discussed in Section 4, while the conclusions and future directions are summarized in Section 5.

2. Data and methodology

2.1. Study areas

For the investigation of the NDVI in Amazon region and the SST of Atlantic sea surface, the following rectangular boxes are selected: from 76°W to 34°W and 7°N to 17°S for the Amazonia NDVI, and from 76°W to 14°W and 25°N to 41°S for the Atlantic SST (see Fig. 1). The selected areas for NDVI and SST are then divided into 87 cells (L1–L110 in Fig. 1) with the size of $3 \times 3°$, and 105 cells (S1–S165 in Fig. 1) with the size of $6 \times 6°$, respectively. L and S denote the land and the sea grids, respectively.

2.2. Spatial characteristics of Amazonian vegetation types

Vegetation type can be defined as a group of plant species sharing the same response to perturbations (e.g., climate factors and fire), and each vegetation type has different physiological characteristics and unique tolerance and adaptation strategies against environmental stresses. Thus, accurate information on the dominant vegetation type in each study grid is essential for the investigation of vegetation greenness (NDVI) change under climate change condition. In this study, we use a global land cover database for the year 2000 from the GLC2000 land cover mapping project (Bartholomé and Belward, 2005), which is based on satellite remote sensing data with a 1-km spatial resolution from the VGETATION sensor on-board SPOT 4. Table 1 lists 22 global land cover types (including 18 vegetation types) of the GLC2000 project.

Regional climate change can affect the structure, function and regional distribution of plant ecosystems, and potentially result in the alternation of vegetation types. In addition, the change in vegetation conditions may be accompanied with distinct environmental responses. In this study, a new index “Vegetation Complexity Index (VCI)” is proposed based on the concept that the spatial distribution of vegetation types in nearby locations can indicate the spatial complexity of vegetation. VCI at a certain location is calculated as the average of the “closeness” values in eight nearest neighboring pixels (Fig. 2). The “closeness” value is specified as 1.0 for the exactly same type of vegetation, 0.7 for the same life form (e.g. trees, shrubs, etc.), 0.3 for the same phenology (e.g. deciduous, evergreen, etc.), and 0.0 for the completely different vegetation types (Table 2). A low value of VCI indicates an unstable plant ecosystem in the succession process when it is most vulnerable to abrupt climate change.

2.3. NDVI and SST data

The monthly 0.5-degree NDVI and 4-km SST data during the period from December 1981 to February 2001 provided by the NOAA/NASA

Table 2
The look-up table according to vegetation types in the determination of closeness value for the calculation of VCI (Fig. 2).

	1	2	3	4	5	6	7	8	9	10	11	12	13	14	15	16	17	18	19	20	21	22
1	1.0	0.3	0.3	0.7	0.3	0.3	0.3	0.3	0.3	0.3	0.0	0.0	0.0	0.0	0.0	0.0	0.3	0.0	0.0	x	x	x
2	0.3	1.0	0.7	0.3	0.7	0.3	0.3	0.3	0.3	0.3	0.0	0.0	0.0	0.0	0.0	0.0	0.3	0.0	0.0	x	x	x
3	0.3	0.7	1.0	0.3	0.7	0.3	0.3	0.3	0.3	0.3	0.0	0.0	0.0	0.0	0.0	0.0	0.3	0.0	0.0	x	x	x
4	0.7	0.3	0.3	1.0	0.3	0.3	0.3	0.3	0.3	0.3	0.0	0.0	0.0	0.0	0.0	0.0	0.3	0.0	0.0	x	x	x
5	0.3	0.7	0.7	0.3	1.0	0.3	0.3	0.3	0.3	0.3	0.0	0.0	0.0	0.0	0.0	0.0	0.3	0.0	0.0	x	x	x
6	0.3	0.3	0.3	0.3	0.3	1.0	0.7	0.7	0.7	0.3	0.0	0.0	0.0	0.0	0.0	0.0	0.3	0.0	0.0	x	x	x
7	0.3	0.3	0.3	0.3	0.3	0.7	1.0	0.7	0.7	0.3	0.0	0.0	0.0	0.0	0.0	0.0	0.3	0.0	0.0	x	x	x
8	0.3	0.3	0.3	0.3	0.3	0.7	0.7	1.0	0.7	0.3	0.0	0.0	0.0	0.0	0.0	0.0	0.3	0.0	0.0	x	x	x
9	0.3	0.3	0.3	0.3	0.3	0.7	0.7	0.7	1.0	0.3	0.0	0.0	0.0	0.0	0.0	0.0	0.3	0.0	0.0	x	x	x
10	0.3	0.3	0.3	0.3	0.3	0.3	0.3	0.3	0.3	1.0	0.0	0.0	0.0	0.0	0.0	0.0	0.3	0.0	0.0	x	x	x
11	0.0	0.0	0.0	0.0	0.0	0.0	0.0	0.0	0.0	0.0	1.0	0.7	0.3	0.3	0.3	0.0	0.0	0.3	0.0	x	x	x
12	0.0	0.0	0.0	0.0	0.0	0.0	0.0	0.0	0.0	0.0	0.7	1.0	0.3	0.3	0.3	0.0	0.0	0.3	0.0	x	x	x
13	0.0	0.0	0.0	0.0	0.0	0.0	0.0	0.0	0.0	0.0	0.3	0.3	1.0	0.7	0.7	0.0	0.0	0.3	0.0	x	x	x
14	0.0	0.0	0.0	0.0	0.0	0.0	0.0	0.0	0.0	0.0	0.3	0.3	0.7	1.0	0.7	0.0	0.0	0.3	0.0	x	x	x
15	0.0	0.0	0.0	0.0	0.0	0.0	0.0	0.0	0.0	0.0	0.3	0.3	0.7	0.7	1.0	0.0	0.0	0.3	0.0	x	x	x
16	0.0	0.0	0.0	0.0	0.0	0.0	0.0	0.0	0.0	0.0	0.0	0.0	0.0	0.0	0.0	1.0	0.3	0.3	0.0	x	x	x
17	0.3	0.3	0.3	0.3	0.3	0.3	0.3	0.3	0.3	0.3	0.0	0.0	0.0	0.0	0.0	0.3	1.0	0.3	0.0	x	x	x
18	0.0	0.0	0.0	0.0	0.0	0.0	0.0	0.0	0.0	0.0	0.3	0.3	0.3	0.3	0.3	0.3	0.3	1.0	0.0	x	x	x
19	0.0	0.0	0.0	0.0	0.0	0.0	0.0	0.0	0.0	0.0	0.0	0.0	0.0	0.0	0.0	0.0	0.0	0.0	1.0	x	x	x
20	x	x	x	x	x	x	x	x	x	x	x	x	x	x	x	x	x	x	x	1.0	x	x
21	x	x	x	x	x	x	x	x	x	x	x	x	x	x	x	x	x	x	x	x	1.0	x
22	x	x	x	x	x	x	x	x	x	x	x	x	x	x	x	x	x	x	x	x	x	1.0

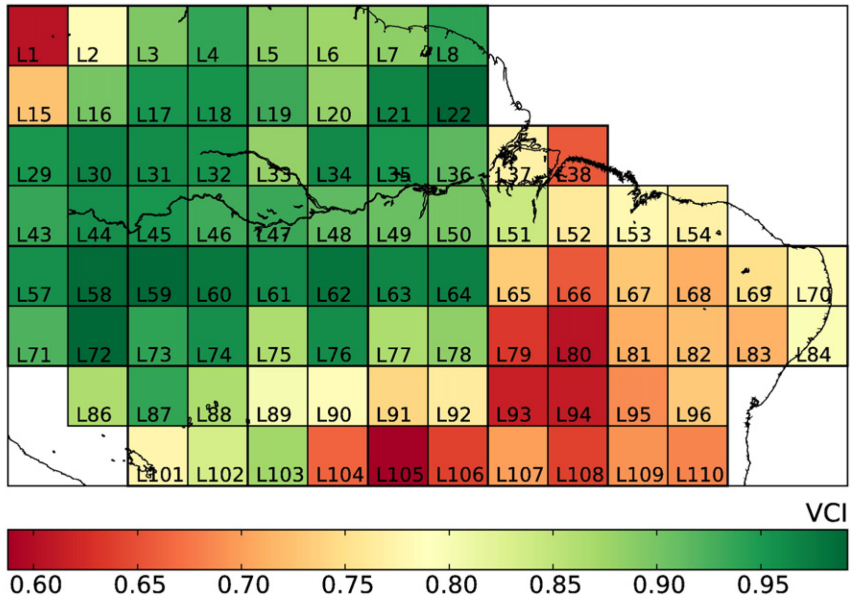

Fig. 3. The contour map of the VCI value of the study area based on the GLC2000 land cover data at 1-km resolution.

Pathfinder Advanced Very-High Resolution Radiometer (AVHRR) are used in this study (McClain et al., 1985; Brown et al., 1985; Kilpatrick et al., 2001). The study period (1981–2001) includes five major ENSO events: 1982–83, 1986–88, 1991–92, 1994–1995 and 1997–98 (Trenberth, 1997; Torrence and Webster, 1999). Even though the seasonal reversal of surface winds is not apparent over the South America, the wind flow in the Amazon region is generally from the tropical Atlantic Ocean with the moisture transport markedly changed between dry and rainy seasons. Therefore, in analyzing the relationships between Amazonian NDVI and Atlantic SST, we choose the DJF-

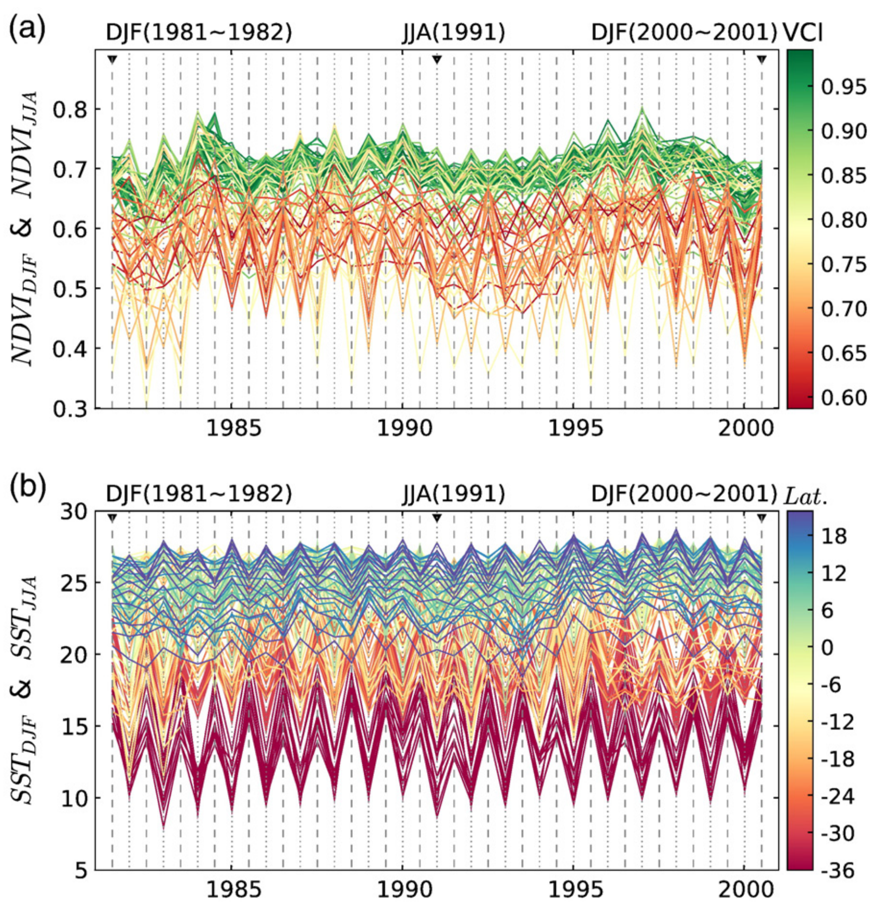

Fig. 4. The 1981–2001 time series of annual DJF- and JJA-averaged (a) NDVI and (b) SST of each land and sea grid box. The color bar in (a) indicates the VCI value of land grid boxes, and the color bar in (b) indicates the latitude of all sea grid boxes.

average (December–January–February) for rainy season and JJA-average (June–July–August) for dry season.

3. The characteristics of Amazonian NDVI and Atlantic SST

3.1. VCI

Based on the vegetation classification map provided by GLC2000, Fig. 3 shows averaged VCI of each grid cell over the study domain. As seen, the Amazon River basin dominated by broadleaf evergreen forest has relatively high VCI, whereas the savanna-dominated area in Northeastern Brazil (L53–54, 67–70, 81–84, and 95–96 in Fig. 3) has relatively lower VCI than Amazon. The neighboring regions of Amazon and Northeastern Brazil have the lowest VCI (Fig. 3). The spatial variation of VCI in the study region indicates different characteristics of the vegetation response to climate change. For example, the low VCI areas consisted of various vegetation types tend to be more vulnerable to sudden environmental change because the plant ecosystem in the successional transition may experience a wide range of stresses. Therefore, the information on the spatial organization of vegetation is important to understand vegetation dynamics (Turner et al., 2007).

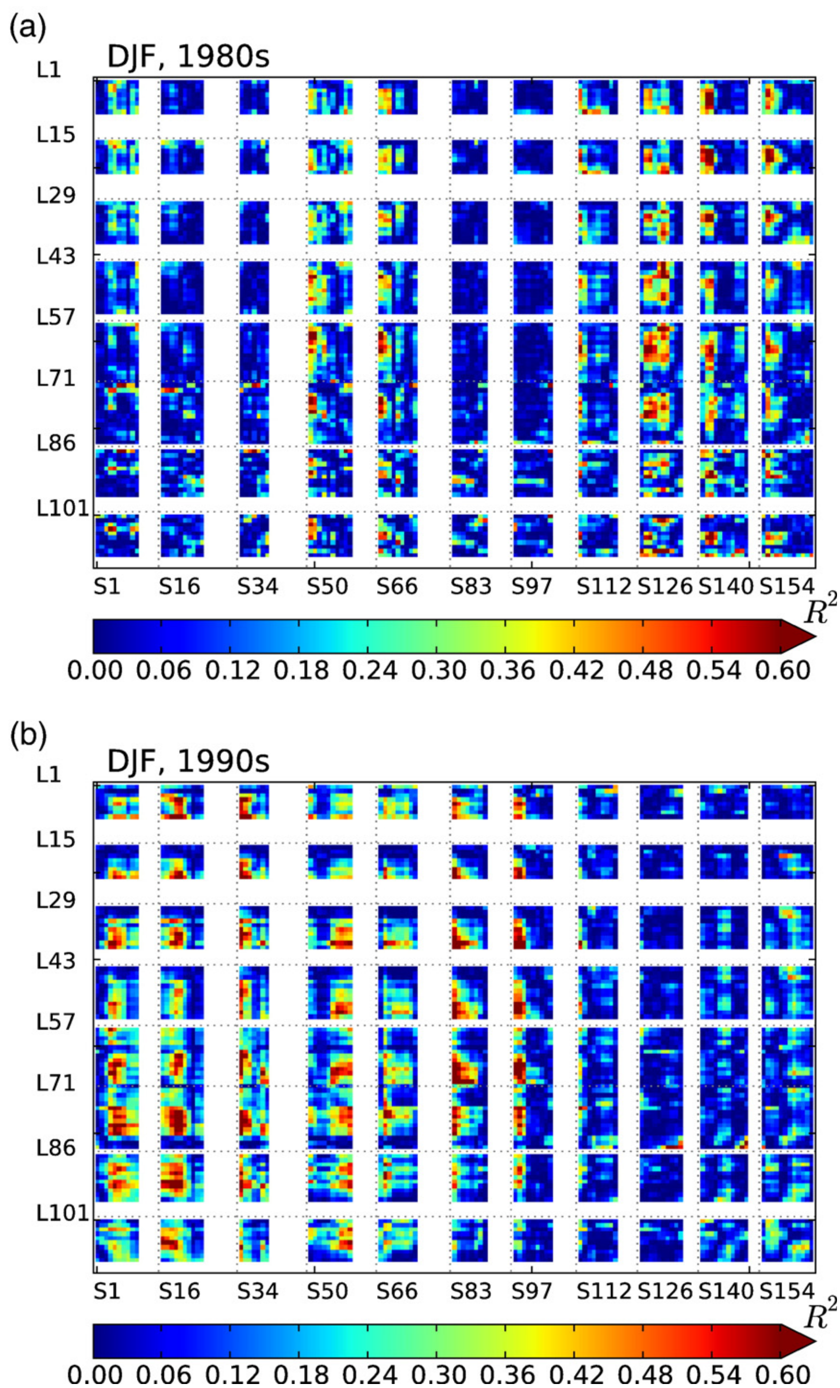

Fig. 5. The coefficient of determination (R^2) between DJF-averaged Amazonian NDVI and Atlantic SST for the period of (a) the 1980s and (b) the 1990s (see the text for the definitions of years).

3.2. Interannual NDVI and SST variation

Fig. 4 shows the interannual variability of DJF- and JJA-averaged NDVI and SST at each grid cell from 1981 to 2001. As seen, the regions with relatively high VCI (dominated by tropical forest) also have higher NDVI compared to the low VCI regions (mixed savanna). The amplitude of seasonal variations of DJF- and JJA-averaged NDVI ($NDVI_{DJF}$ and $NDVI_{JJA}$) in low VCI regions is larger than that in high VCI regions. Moreover, the interannual NDVI fluctuation in high VCI regions is rather small during 1991–1994. In general, $NDVI_{JJA}$ is larger (smaller) than $NDVI_{DJF}$ in high (low) VCI regions, because Amazonian tropical trees are strongly controlled by the variation of radiation in dry (JJA) and rainy (DJF) seasons (Huete et al., 2006). In 1989, $NDVI_{JJA}$ has the largest difference during the 1981–2001 period between high and low VCI regions. Remarkable NDVI changes during 1980s are the large $NDVI_{DJF}$ in 1984–1985 and $NDVI_{JJA}$ in 1984 for higher VCI regions, and $NDVI_{DJF}$ in 1982–1983 has the lowest value among high VCI regions. During 1990s, $NDVI_{JJA}$ in 1997 in high VCI regions has the largest value, whereas $NDVI_{JJA}$ in 2000 has the lowest value for most of the study areas.

As the region of interest for SST moves from north to south, the more interannual SST variations are found. Moreover, the SST variations of the regions north or south to the equator have different characteristics. The SST north to the equator is warmer than that south to equator, and SST_{DJF} in the regions north (south) to the equator is smaller (larger) than SST_{JJA}. The interannual variability of SST_{DJF} and SST_{JJA} during the study period (1981–2001) appears to be relatively small compared to the interannual variability of NDVI.

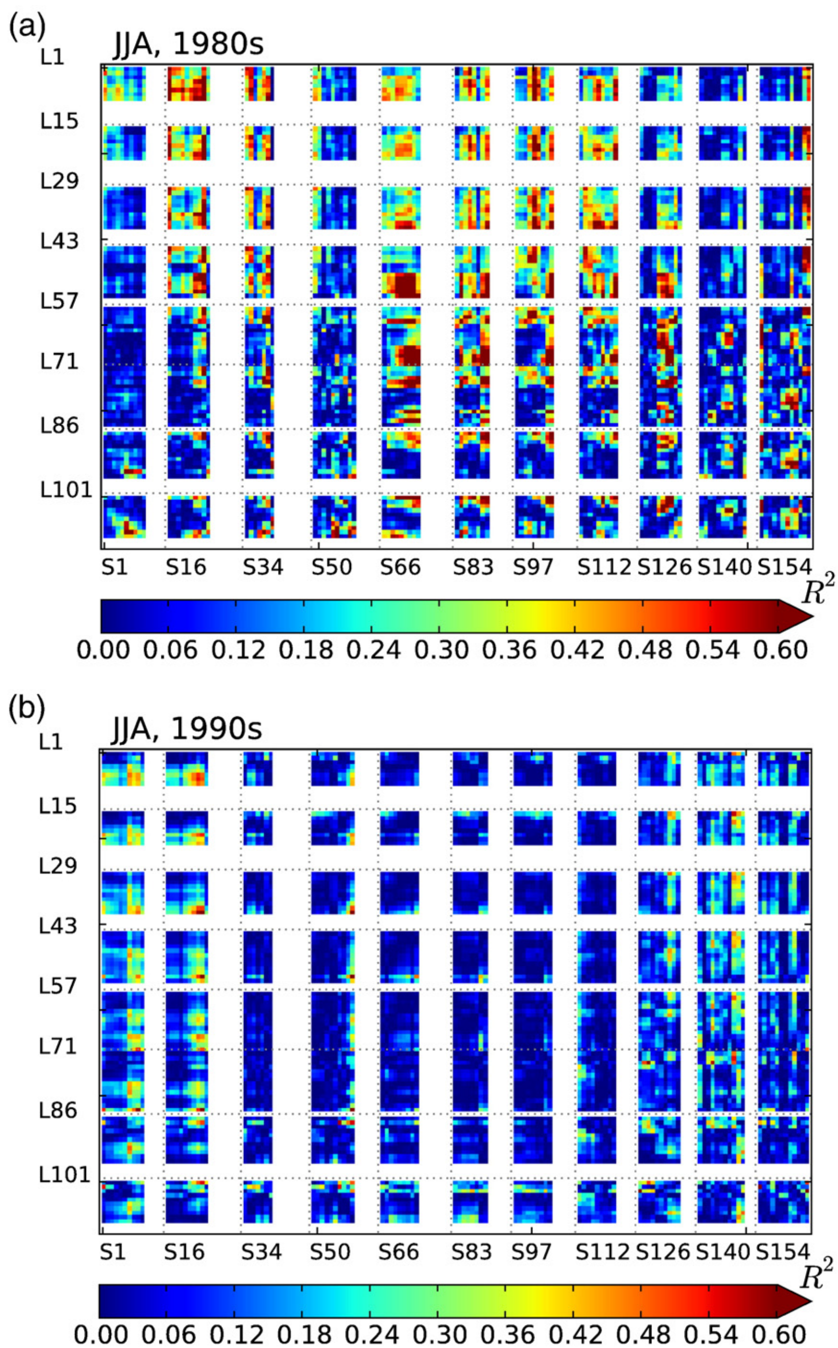

Fig. 6. Same as Fig. 5, but for JJA-averaged Amazonian NDVI and Atlantic SST.

4. The relationship between Amazonian NDVI and Atlantic SST

The matrix of the coefficient of determination (R^2) between NDVI and SST for all the grid pairs over the study domain is plotted in Figs. 5 and 6, for the period of 1981–1990 and 1991–2001 (hereafter as 1980s and 1990s), respectively. As observed, strong correlation can be found between certain land and sea grid cells for both study periods. Meanwhile, the spatial distribution patterns of relatively high correlation are different for the four cases examined (DJF and JJA in 1980s and 1990s). For the DJF in 1980s, the western areas of both the equatorial Atlantic sea surface and South Atlantic are the two regions where significant correlation is found between SST_{DJF} and $NDVI_{DJF}$. For the DJF in 1990s, the majority of the study areas in Amazon show high correlations with the SST of the entire Atlantic Ocean (except for the part south of 10°S). On the other hand, for the JJA in 1980s, the pattern of correlation is similar to the distribution of DJF in 1990s (Fig. 6a). However, the south part of the entire study area of land has relatively stronger (weaker) correlation with the Atlantic SST of around 20°S (20°N). Moreover, the correlation coefficient for JJA in 1990s is generally the lowest among the four cases examined.

Figs. 7 and 8 present the highest correlation coefficient (R^2) between NDVI and SST. As can be observed, the spatial pattern of the highest correlation differs in all the four cases examined. High interannual correlations of $NDVI_{DJF}$ and SST_{DJF} in rainy season are distributed over the western part of the study area in 1980s (Fig. 7a), and it slightly shifts to east where it is the transitional region with high VCI between tropical forest and savanna. The highest correlation between $NDVI_{JJA}$ and SST_{JJA} shows extremely different situations in 1980s and 1990s (Fig. 7). For 1980s, high correlation was observed over most of land regions, while consistently low correlation was found for 1990s (Fig. 8). The different spatial distribution shown in Figs. 7 and 8 was possibly caused by different vegetated conditions under varying rainfall and atmospheric circulation conditions.

Notice that the spatial distribution of the highest correlation for DJF (JJA) in 1980s and 1990s mostly does not overlap. For a certain cell with a high correlation in 1980s, it is often accompanied with a low

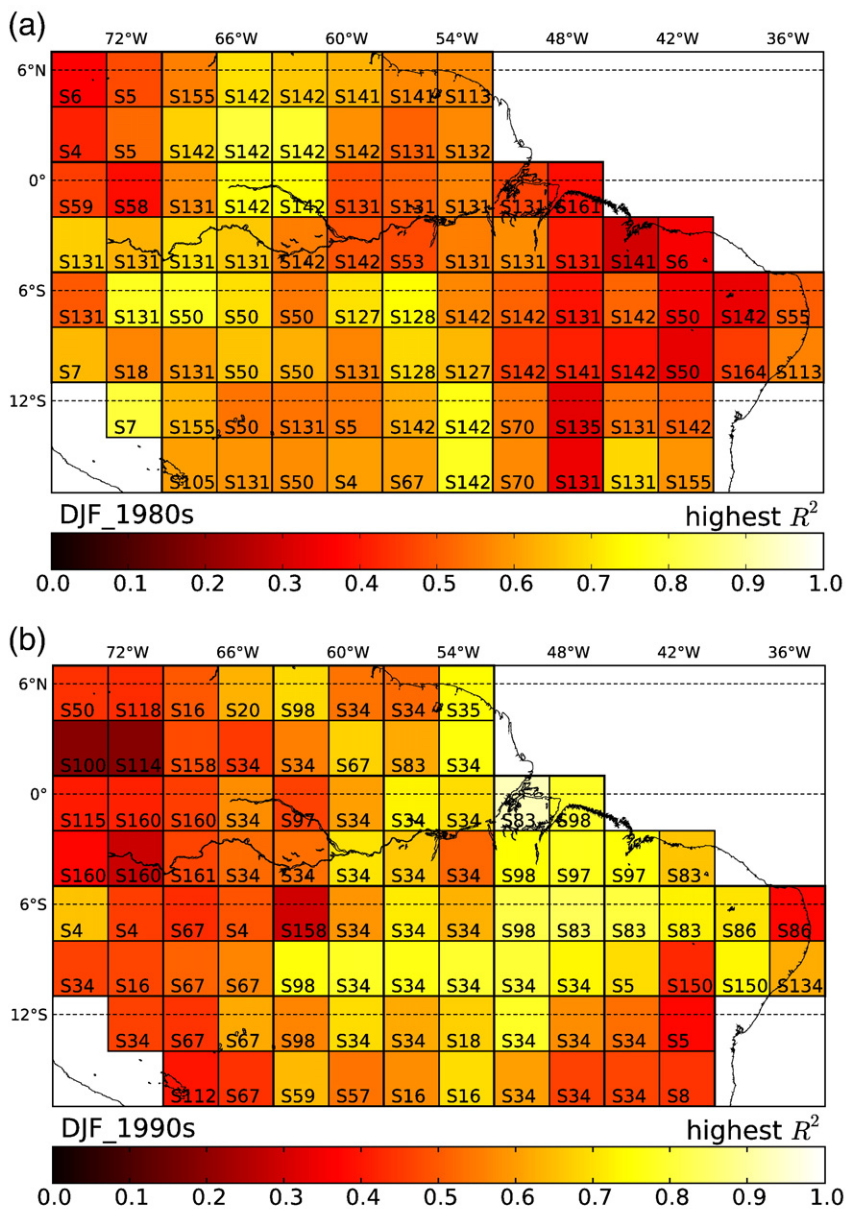

Fig. 7. Colored boxes in Amazon region represent the highest coefficient of determination (R^2) between DJF-averaged Amazonian NDVI and Atlantic SST. The numbering on each land grid box indicates the numbering of the sea grid box with the highest correlation: (a) for the 1980s and (b) for the 1990s.

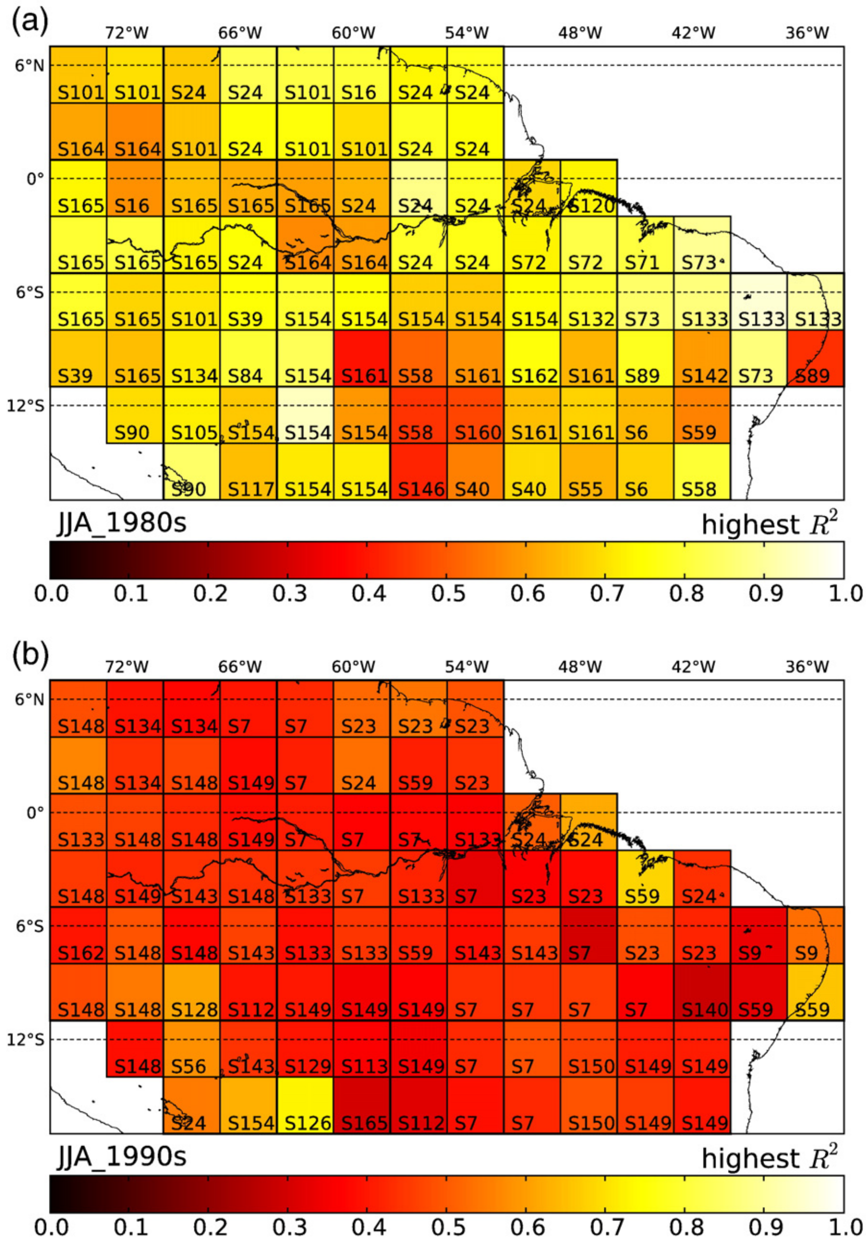

Fig. 8. Same as Fig. 7, but for JJA-averaged Amazonian NDVI and Atlantic SST.

correlation in 1990s. Two land grid cells (L63 for DJF and L53 for JJA) were selected to examine their highest correlations with Atlantic SST (Fig. 9). As shown in Fig. 9, the correlation between L63 and S128 for the DJF in 1980s is negative. However, most of the data points are clustered around 25 °C (SST) and 0.68 (NDVI), indicating the generally small interannual variability of both NDVI and SST, but with two distinct outliners corresponding to 1984–85 and 1982–83, respectively. In this case, linear regression line primarily reflects the sudden change in the interannual variation of both SST and NDVI due to strong external forcing. For the rest of Fig. 9, fairly good positive correlation between NDVI and SST can be observed. Indeed, Myneni et al. (2007) have shown the positive correlation between leaf area index (LAI) and solar radiation for several regions in the Amazon.

Generally, the relationship between NDVI and climatic factors (e.g., rainfall) is usually studied by examining the correlation between them (e.g., Camberlin et al., 2007), as shown in Figs. 5 and 6 of this study. In addition, the correlation with certain time lags also has to be taken into account because of the delayed responses to environmental forcing (e.g., soil moisture) and physiological tolerance of vegetation (Nicholson et al., 1990; Oesterheld et al., 2001; Martiny et al., 2005). In Figs. 10 and 11, the correlations between monthly NDVI and SST with a two-month and one-year lag, respectively, are considered. As seen, the correlation with a two-month lag between $NDVI_{DJF}$ and SST_{OND} (i.e. the average SST from October to December) is high, particularly between the eastern part of land regions and the equatorial Atlantic Ocean (Fig. 10a). The correlation coefficient with one-year lag (between SST_{DJF} of previous year and $NDVI_{DJF}$ of current year), as shown in Fig. 11a, is stronger than the zero-lag correlation during the same period (Fig. 5a). However, while the correlation with time lag is evident in rainy season DJF (Figs. 10a and 11a), it is generally weak in dry season JJA (Figs. 10b and 11b).

5. Conclusions

Climate model projections for the future climate and vegetation condition usually contain a significant amount of uncertainties due to

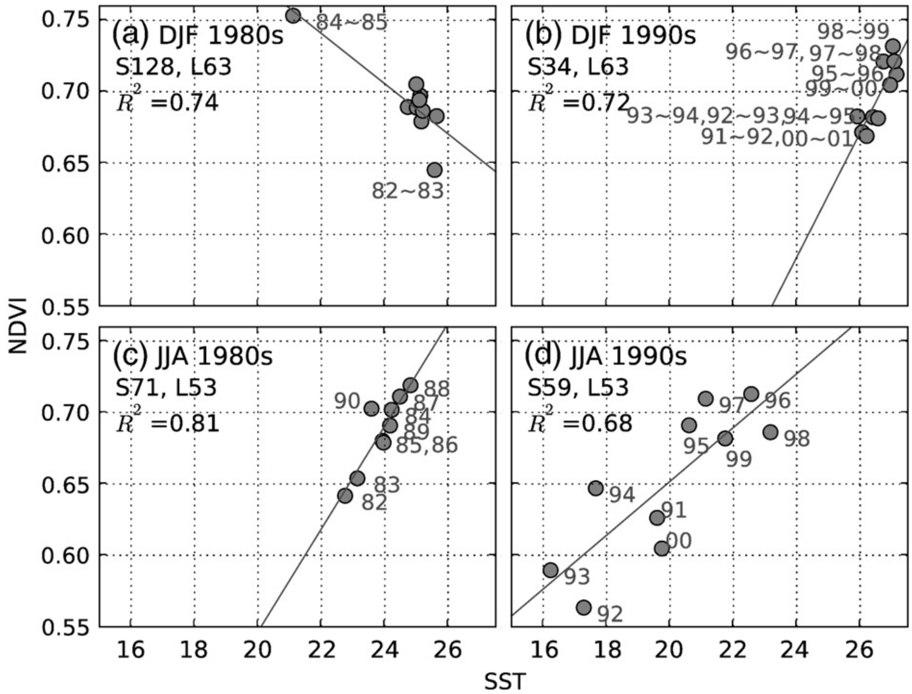

Fig. 9. Plot of Atlantic SST versus Amazonia NDVI as well as their linear regression in four selected land–sea grid pairs.

complex regional variability in the integrated atmosphere–biosphere system (IPCC, 2007). Accordingly, better understanding of the variations of climate and vegetation in Amazon by using the data from in-situ observations or satellite remote sensing should lead to an improved projection of the impacts of future climate change on the Amazon vegetation.

In this study, the effect of Atlantic SST on the spatial and temporal change of the Normalized Difference Vegetation Index (NDVI) in the Amazonian region is examined by using satellite remote sensing data for the period of 1981–2001. We found that (1) a strong correlation exists between NDVI and SST in certain regions of Amazon and the Atlantic Ocean, as shown respectively for two analyzed periods (1980s and 1990s); (2) the correlations between Amazon NDVI and Atlantic SST with a two-month or one-year lag (i.e., NDVI lags behind SST) are both strong in the DJF (rainy season) interannual variations. Despite these findings, the mechanisms behind the identified correlations remained unclear primarily because of the following complexities involved in the ocean–atmosphere–biosphere system. First, the past vegetation condition is a critical starting point for potential vegetation change (Myneni et al., 1996; Batista et al., 1997), which could result in different vegetation response to an identical set of environmental changes. Second, Amazonian aerosol particles released by fires are important as a climate regulator because it can inhibit the formation of clouds, thus reducing rainfall with water vapor transported from the Atlantic Ocean (Koren et al., 2004). Third, the variation of local land surface temperature induced by vegetated and land cover change will drive large-scale atmospheric moisture transport because the increased gradient of land–ocean temperature can lead to a seasonal change of atmospheric circulation patterns (Wang and Fu, 2007).

Indentifying the characteristics of NDVI variability to climatic conditions in the Amazon region may provide important clues toward the understanding of vegetation variability, terrestrial carbon cycle, and eco-hydrological processes (Skole and Tucker, 1993; Roberts et al., 2003). Therefore, our investigation of the linkage between Amazon NDVI and Atlantic SST can help interpret and validate climate model simulations, particularly for the processes associated with the physiological effects of terrestrial ecosystems in the global water and carbon cycles (Cao and Woodward, 1998; Betts et al., 2007). In addition, the expectation of how Amazonian ecosystem will respond to future climate change is important for climate model simulations. Therefore, more similar analyses as demonstrated in this study by using observed data and modelling experiments across a wide range of spatial and time scale are necessary to predict the fate of Amazonian rainforest under the future global warming.

Acknowledgements

This study was funded by Grants-in-Aid for Scientific Research from the Japan Society for the Promotion of Science (19106008) and Postdoctoral Fellowship of the Japan Society for the Promotion of Science for Foreign Researchers (#21-09289).

References

Bartholomé, E., Belward, A.S., 2005. GLC2000: a new approach to global land cover mapping from Earth observation data. Int. J. Remote Sens. 26, 1959–1977.

Batista, G.T., Shimabukuro, Y.E., Lawrence, W.T., 1997. The long-term monitoring of vegetation cover in the Amazonian region of northern Brazil using NOAA-AVHRR data. Int. J. Remote Sens. 18, 3195–3210.

Betts, R.A., Boucher, O., Collins, M., Cox, P.M., Falloon, P.D., Gedney, N., Hemming, D.L., Huntingford, C., Jones, C.D., Sexton, D.M.H., Webb, M.J., 2007. Projected increase in continental runoff due to plant responses to increasing carbon dioxide. Nature 448, 1037–1041.

Bonan, G.B., 2002. Ecological Climatology. Cambridge University Press, New York.

Brown, O.W., Brown, J.W., Evans, R.H., 1985. Calibration of advanced very high resolution radiometer observations. J. Geophys. Res. 90. doi:10.1029/JC090iC06p11667.

Camberlin, P., Martiny, N., Philippon, N., Richard, Y., 2007. Determinants of the interannual relationships between remote sensed photosynthetic activity and rainfall in tropical Africa. Rem. Sens. Environ. 106, 199–216.

Cao, M.K., Woodward, F.I., 1998. Dynamic responses of terrestrial ecosystem carbon cycling to global climate change. Nature 393, 249–252.

Cox, P.M., Betts, R.A., Jones, C.D., Spall, S.A., Totterdell, I.J., 2000. Acceleration of global warming due to carbon-cycle feedbacks in a coupled climate model. Nature 408, 184–187.

Cox, P.M., Betts, R.A., Collins, M., Harris, C., Huntingford, C., Jones, C.D., 2004. Amazonian forest dieback under climate-carbon cycle projections for the 21st century. Theor. Appl. Climatol. 78, 137–156.

Eagleson, P.S., 1986. The emergence of global-scale hydrology. Water Resour. Res. 22, 6S–14S.

Enfield, D.B., 1996. Relationships of inter-American rainfall to tropical Atlantic and Pacific SST variability. Geophys. Res. Lett. 23, 3305–3308.

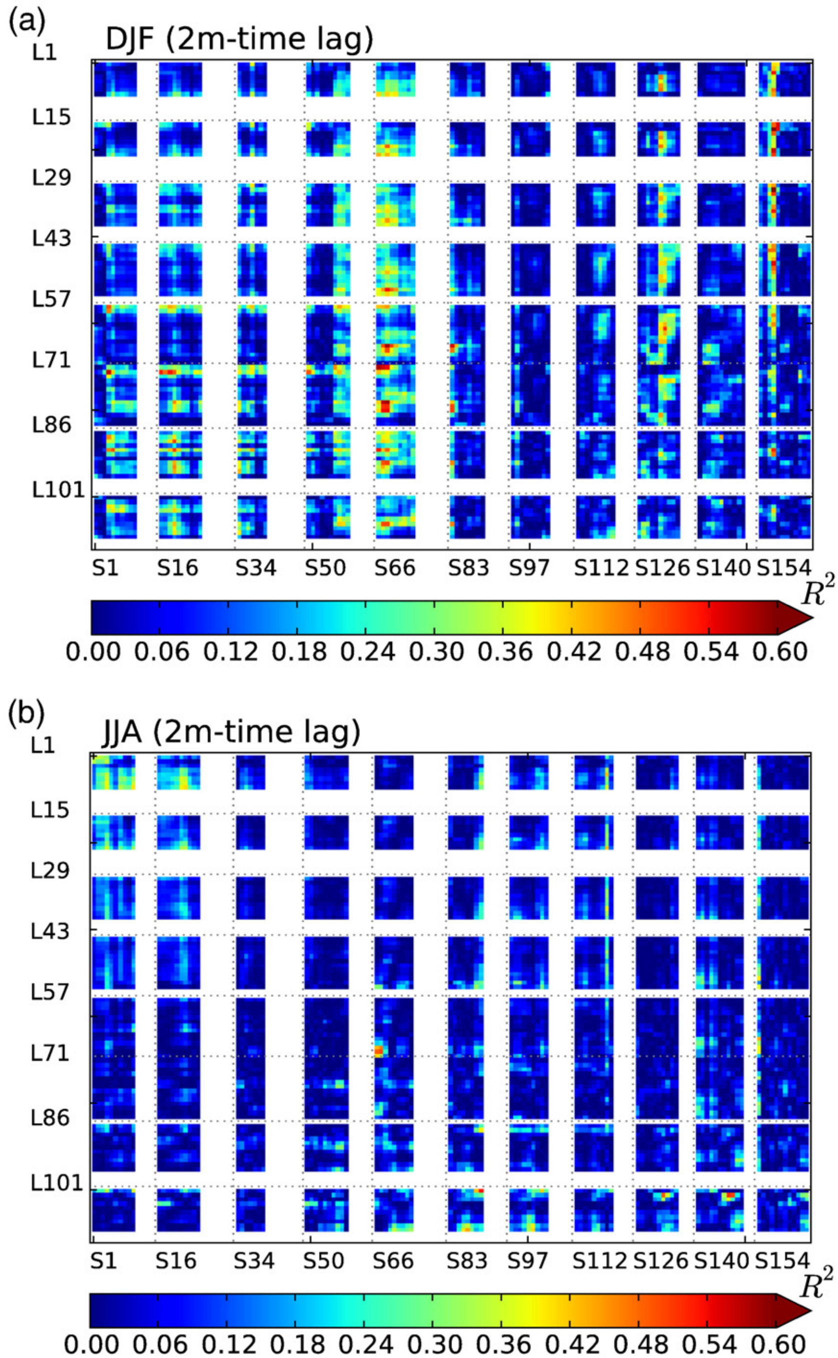

Fig. 10. The coefficient of determination (R^2) between Amazonian NDVI and Atlantic SST during 1981–2001 for (a) $NDVI_{DJF}$ and (b) $NDVI_{JJA}$ with a 2-month lag of Amazonia NDVI behind Atlantic SST.

Good, P., Lowe, J.A., Collins, M., Moufouma-Okia, W., 2008. An objective tropical Atlantic sea surface temperature gradient index for studies of south Amazon dry-season climate variability and change. Phil. Trans. R. Soc. B 363, 1761–1766.

Harris, P.P., Huntingford, C., Cox, P.M., 2008. Amazon basin climate under global warming: the role of the sea surface temperature. Phil. Trans. R. Soc. B. 363, 1753–1759.

Huete, A.R., Didan, K., Shimabukuro, Y.E., Ratana, P., Saleska, S.R., Hutyra, L.R., Yang, W., Nemani, R.R., Myneni, R., 2006. Amazon rainforests green-up with sunlight in dry season. Geophys. Res. Lett. 33, L06405. doi:10.1029/2005GL025583.

Intergovernmental Panel on Climate Change (IPCC) Climate change, 2007. Contribution of working group 1 to the Fourth Assessment Report of the Intergovernmental Panel on Climate Change. Cambridge University Press 2007. Cambridge University Press, Cambridge, UK.

International Geosphere-Biosphere Programme (IGBP), 1997. The terrestrial biosphere and global change: Implications for natural and managed ecosystems. A synthesis of GCTE and related research. In: Walker, B., Steffen, W. (Eds.), IGBP Science No.1, IGBP Secretariat. The Royal Swedish Academy of Sciences, Stockholm, Sweden.

Kilpatrick, K.A., Podesta, G.P., Evans, R., 2001. Overview of the NOAA/NASA Advanced Very High Resolution Radiometer Pathfinder algorithm for sea surface temperature and associated matchup database. J. Geophys. Res. 106, 9179–9197.

Knight, J.R., Folland, C.K., Scaife, A.A., 2006. Climate impacts of the Atlantic multidecadal oscillation. Geophys. Res. Lett. 33, L17706. doi:10.1029/2006GL026242.

Koren, I., Kaufman, Y.J., Remer, J.A., Martins, J.V., 2004. Measurement of the effect of Amazon smoke on inhibition of cloud formation. Science 27, 1342–1345.

Li, W.H., Dickinson, R.E., Fu, R., Niu, G.-Y., Yang, Z.-L., Canadell, J.G., 2007. Future precipitation changes and their implications for tropical peatlands. Geophys. Res. Lett. 34, L01403. doi:10.1029/2006GL028364.

Los, S.O., Collatz, G.J., Bounoua, L., Sellers, P.J., Tucker, C.J., 2001. Global interannual variations in sea surface temperature and land surface vegetation, air temperature, and precipitation. J. Climate 14, 1535–1549.

Lovejoy, T.E., Hannah, L., 2004. Climate Change and Biodiversity. Yale Academic Press, New Haven.

Marengo, J.A., 1992. Interannual variability of surface climate in the Amazon Basin. Int. J. Climatol. 12, 853–863.

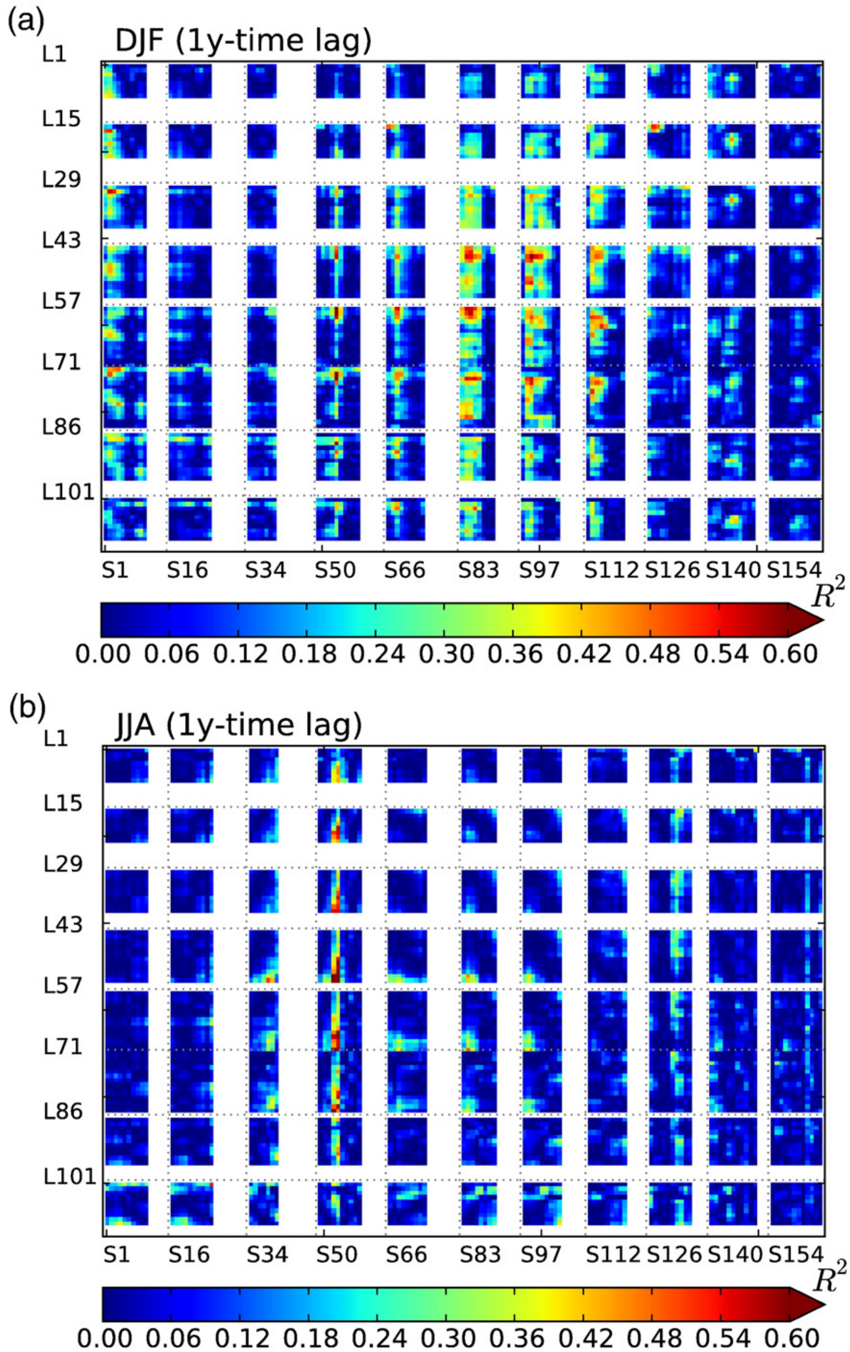

Fig. 11. Same as Fig. 10, but with a 1-year lag of Amazonia NDVI behind Atlantic SST.

Marengo, J.A., Liebmann, B., Kousky, V.E., Filizola, N.P., Wainer, I.C., 2001. Onset and end of the rainy season in the Brazilian Amazon basin. J. Climate 14, 833–852.

Martiny, N., Richard, Y., Camberlin, P., 2005. Interannual persistence effects in vegetation dynamics of semi-arid Africa. Geophys. Res. Lett. 32, L24403. doi:10.1029/2005GL024634.

McClain, E.P., Pichel, W.G., Walton, C.C., 1985. Comparative performance of AVHRR-based multichannel sea surface temperatures. J. Geophys. Res. 90, 11587–11601.

Myneni, R.B., Los, S.O., Tucker, C.J., 1996. Satellite-based identification of linked vegetation index and sea surface temperature anomaly area from 1982–1990 for Africa, Australia and South America. Geophys. Res. Lett. 23, 729–732.

Myneni, R.B., Yang, W., Nemani, R.R., Huete, A.R., Dickinson, R.E., Knyazikhin, Y., Didan, K., Fu, R., Negrón Juárez, R.I., Saatchi, S.S., Hashimoto, H., Ichii, K., Shabanov, N.V., Tan, B., Ratana, P., Privette, J.L., Morisette, J.T., Vermote, E.F., Roy, D.P., Wolfe, R.E., Friedl, M.A., Running, S.W., Votava, P., El-Saleous, N., Devadiga, S., Su, Y., Salomonson, V.V., 2007. Large seasonal swings in leaf area of Amazon rainforests. PNAS 104, 4820–4823.

Nemani, R.R., Keeling, C.D., Hashimoto, H., Jolly, W.M., Piper, S.C., Tucker, C.J., Myneni, R.B., Running, S.W., 2003. Climate-driven increases in global terrestrial net primary production from 1982 to 1999. Science 300, 1560–1563.

Nepstad, D.C., de Carvalho, C.R., Davidson, E.A., Jipp, P.H., Lefebvre, P.A., Negreiros, G.H., Dasilva, E.D., Stone, T.A., Trumbore, S.E., Vieira, S., 1994. The role of deep roots in the hydrological and carbon cycles of Amazonian forest and pastures. Nature 372, 666–669.

Nicholson, S., Davenport, M., Malo, A.R., 1990. A comparison of the vegetation response to rainfall in the Sahel and East Africa, using Normalized Difference Vegetation Index from NOAA AVHRR. Climatic Change 17, 209–241.

Oesterheld, M., Loreti, J., Semmartin, M., Sala, O.E., 2001. Inter-annual variation in primary production of a semi-arid grassland related to previous-year production. J. Veg. Sci. 12, 137–142.

Phillips, O.L., Aragao, L.E.O.C., Lewis, S.L., Fisher, J.B., Lloyd, J., Lopez-Gonzalez, G., Malhi, Y., Monteagudo, A., Peacock, J., Quesada, C.A., van der Heijden, G., Almeida, S., Amaral, I., Arroyo, L., Aymard, G., Baker, T.R., Banki, O., Blanc, L., Bonal, D., Brando, P., Chave, J., de Oliveira, A.C.A., Cardozo, N.D., Czimczik, C.I., Feldpausch, T.R., Freitas, M.A., Gloor, E., Higuchi, N., Jimenez, E., Lloyd, G., Meir, P., Mendoza, C., Morel, A., Neill, D.A., Nepstad, D., Patino, S., Penuela, M.C., Prieto, A., Ramirez, F., Schwarz, M., Silva, J., Silveira, M., Thomas, A.S., Steege, H.T., Stropp, J., Vasquez, R., Zelazowski, P., Davila, E.A., Andelman, S., Andrade, A., Chao, K.-J., Erwin, T., Di Fiore, A., Keeling, E.H. C.H., Killeen, T.J., Laurance, W.F., Cruz, A.P., Pitman, N.C.A., Vargas, P.N., Ramirez-

Angulo, H., Rudas, A., Salamao, R., Silva, N., Terborgh, J., Torres-Lezama, A., 2009. Drought sensitivity of the Amazon rainforest. Science 323, 1344–1347.
Rao, V.B., Cavalcanti, I., Hada, K., 1996. Annual variation of rainfall over Brazil and water vapour characteristics over South America. J. Geophys. Res. 101, 26539–26551.
Roberts, D.A., Keller, M., Soares, J.V., 2003. Studies of land-cover, land-use, and biophysical properties of vegetation in the Large Scale Biosphere Atmosphere experiment in Amazônia. Rem. Sens. Environ. 87, 377–388.
Ronchail, J., Cochonneau, G., Molinier, M., Guyot, J.-L., de M. CHAVES, A.G., Guimarães, V., de Oliveira, E., 2002. Interannual rainfall variability in the Amazon basin and sea-surface temperatures in the equatorial Pacific and the tropical Atlantic Oceans. Int. J. Climatol. 22, 1663–1686.
Saleska, S.R., Miller, S.D., Matross, D.M., Goulen, M.L., Wofsy, S.C., da Rocha, H.R., de Camargo, P.B., Crill, P., Daube, B.C., de Freitas, H.C., Hutyra, L., Keller, M., Kirchhoff, V., Menton, M., Munger, J.W., Pyle, E.H., Rice, A.H., Silva, H., 2003. Carbon in Amazon forests: unexpected seasonal fluxes and disturbance-induced losses. Science 302, 1554–1557.
Skole, D., Tucker, C., 1993. Evidence for tropical deforestation, fragmented habitat, and adversely affected habitat in the Brazilian Amazon: 1978–1988. Science 260, 1905–1910.
Smith, K., Gholz, H.L., de Assis Oliveira, F., 1998. Litterfall and nitrogen–use efficiency of plantations and primary forest in the eastern Brazilian Amazon. For. Ecol. Manage. 109, 209–220.
Torrence, C., Webster, P.J., 1999. Interdecadal changes in the ENSO-monsoon system. J. Climate 12, 2679–2690.
Trenberth, K.E., 1997. The definition of El Niño. Bull. Amer. Meteor. Soc. 78, 2771–2777.
Turner, B.L., Lambin, E.F., Reenberg, A., 2007. The emergence of land change science for global environmental change and sustainability. PNAS 104, 20666–20671.
Wang, H., Fu, R., 2007. The influence of Amazon rainfall on the Atlantic ITCZ through convectively coupled Kelvin waves. J. Climate 20, 1188–1201.
Zeng, N., Yoon, J., Marengo, J., Subamaniam, A., Nobre, C., Mariotti, A., Neelin, J.D., 2008. Causes and impact of the 2005 Amazon drought. Environ. Res. Lett. 3, 014002. doi:10.1088/1748-9326/3/1/014002.